Search and Characterization of ITM2A as a New Potential Target for Brain Delivery

Céline Cegarra (celine.cegarra@sanofi.com)
Sanofi-Aventis Recherche Developpement Chilly-Mazarin Longjumeau https://orcid.org/0000-0002-1710-9796

Catarina Chaves
Sanofi-Aventis Recherche Développement Chilly-Mazarin: Sanofi-Aventis Recherche Developpement Chilly-Mazarin Longjumeau

Catherine Déon
Sanofi-Aventis Recherche Développement Chilly-Mazarin: Sanofi-Aventis Recherche Developpement Chilly-Mazarin Longjumeau

Tuan Minh Do
Sanofi-Aventis Recherche Développement Chilly-Mazarin: Sanofi-Aventis Recherche Developpement Chilly-Mazarin Longjumeau

Bruno Dumas
Sanofi-Aventis Recherche et Développement Vitry-sur-Seine: Sanofi-Aventis Recherche et Developpement Vitry-sur-Seine Alfortville

André Frenzel
Universität Braunschweig: Technische Universitat Braunschweig

Philip Kuhn
Universität Braunschweig: Technische Universitat Braunschweig

Valérie Roudieres
Sanofi-Aventis Recherche Développement Chilly-Mazarin: Sanofi-Aventis Recherche Developpement Chilly-Mazarin Longjumeau

Jean-Claude Guillemot
Sanofi-Aventis Recherche Développement Chilly-Mazarin: Sanofi-Aventis Recherche Developpement Chilly-Mazarin Longjumeau

Dominique Lesuisse
Sanofi-Aventis Recherche Développement Chilly-Mazarin: Sanofi-Aventis Recherche Developpement Chilly-Mazarin Longjumeau

---

Research

Keywords: Blood Brain Barrier, ITM2A, antibodies, transcytosis

Posted Date: December 3rd, 2021

DOI: https://doi.org/10.21203/rs.3.rs-1125315/v1

Abstract

Background

Integral membrane protein 2A (ITM2A) is a transmembrane protein whose function is not well described. This target was identified as highly enriched in human brain vs peripheral endothelial cells by transcriptomic and proteomic studies during the European Collaboration on the Optimization of Macromolecular Pharmaceutical Innovative Medicines Initiative (COMPACT IMI) consortium. The object of the present paper is to report the work we have undertaken to characterize this protein as a potential brain delivery target.

Methods

A series of ITM2A constructs, cell lines and specific anti-human and mouse ITM2A antibodies were generated. Binding and internalization in Human Embryonic Kidney 293 (HEK293) cells overexpressing ITM2A and in brain microvascular endothelial cells from mouse and non-human primate (NHP) were performed with these tools. The best antibody was evaluated in an in vitro human blood brain barrier (BBB) model and in a mouse in vivo pharmacokinetic study to validate blood brain barrier crossing.

Results

Antibodies specifically recognizing extracellular parts of ITM2A or tags inserted in its extracellular domain showed selective binding and uptake in ITM2A-expressing cells. However, despite high RNA expression in mouse and human microvessels, this protein, is rapidly downregulated upon endothelial cells culture, probably explaining why transcytosis could not be evidenced in vitro. An attempt to directly demonstrate in vivo transcytosis in mice turned out unconvincing, using a cross reactive anti ITM2A antibody on one hand and in vivo phage panning of an anti ITM2A phage library on the other hand.

Conclusions

The present article describes the work we have undertaken to explore the potential of ITM2A as target to mediate transcytosis through BBB. This work highlights the multiple challenges linked to the identification of new brain delivery targets.

Background

Brain is a highly protected tissue. The endothelial cells lining the blood vessels that are at the interface of blood and brain are different than the peripheral endothelial cells, and as opposed to them are extremely tight, non-fenestrated and equipped with many efflux systems. This blood brain barrier is only permeable to very small lipophilic compounds but is actively preventing most molecules to enter and in particular

large or polar molecules such as biotherapeutics and antibodies(1, 2). This explains why some enormous medical needs remain to be addressed in particular for targets for which biologics are the main modality in therapeutic area such as neurosciences, oncology (e.g. central nervous system (CNS) lymphoma or glioblastoma) or rare diseases. For instance, the use of therapeutic antibodies for CNS disorders such as Alzheimer's, Parkinson's, Huntington's diseases or brain cancers has been very limited so far(3) owing to the presence of the BBB. This is also explaining why so few biologics are in development in CNS. The biologics that are on the market in neurology are most certainly acting peripherally (or else given intrathecally)(4). Therefore, strategies to increase brain exposure of biotherapeutics are key to the success of biotherapeutics in this area.

So far, the most successful strategy to carry biotherapeutics to the brain using systemic route has been making use of a ligand or antibody against a receptor-mediated transcytosis (sometimes referred to as the 'Trojan horse' approach). Several receptors such as insulin(5), transferrin(6), lipoprotein-related proteins(7, 8), low density lipoprotein(9) or Insulin-like Growth Factor 1 (10) receptors have been used. Several challenges however remain in the field. One of them is linked to the fact that all these receptors are ubiquitously expressed. So far, no brain-specific receptor capable of mediating such transcytosis has been discovered.

During the COMPACT IMI consortium (https://www.imi.europa.eu/projects-results/project-factsheets/compact) an approach integrating different omics levels of proteomic, MicroArray and RNA sequencing approaches was engaged from human primary endothelial cells from brain, liver and lung aimed at identifying candidate membrane proteins highly enriched in brain vs liver or lung(11). The resulting over 60000 RNA's were then processed through several filters, downsizing to mRNA's not detected at all in liver and/or lung or with high differential level in brain, mRNA's with mostly transmembrane expression, association to the BBB vasculature, expression and selectivity comparable between rodents and humans and high degree of conservation between orthologs. This led to a few mRNA's such as basigin (12) and Low-density lipoprotein receptor-related protein 8 (LRP8)(13) already reported as brain transport mechanisms validating therefore the approach. ITM2A was identified among these mRNA's.

ITM2A (alias E25A or BRICD2A) is a 263-amino acid protein with a single transmembrane domain(14). Its ubiquitous expression is higher in thymus where it was shown to be an activation marker in thymocyte development(15). ITM2A is mainly believed to be associated with cell differentiation during myogenesis(16, 17), chondrogenesis(18–22) and odontogenesis(23). The overall homology between mouse and human is more than 95% in the extracellular domain(24). The protein has a motopsin-binding Brichos domain within the COOH-terminal extracellular domain(25) whose significance is poorly understood(25). Brichos domains appear to bear a chaperone function in different biological situations and particularly bind amyloid fibrils (26). Recently ITM2A expression was shown to negatively regulate autophagic flux by inhibiting lysosomal function through physical interaction with vacuolar Adenosyl Tri Phosphatase(27).

Expression in mouse and human brain has been reported to be homogenous in all brain (Protein Atlas ITM2A) and quite specific of endothelial cells vs neurons, microglia, oligodendrocytes or astrocytes as shown in brain RNA seq database (Fig. 1). In fact, it is referred to as an endothelial cell-specific gene(28). An analysis of five human and murine cell type-specific transcriptome-wide RNA expression data sets that were generated within the past several years also identified ITM2A as one of the top expressed genes in endothelial cells(29). A recent single cell RNA seq analysis of 20 organs in mice also established the ITM2A gene specific for brain endothelial cells(30).

Two precedents point to specific association of ITM2A with the blood brain barrier. ITM2A was identified as microvasculature specific through the screening of subtractive cDNA libraries from rat brain capillaries versus kidney/liver on one hand(31, 32) and from porcine brain and aortic endothelial cells on the other hand(33). In addition, the expression of ITM2A found in freshly isolated porcine Brain Microvascular Endothelial Cells (BMEC) was shown to be lost upon culture similarly to some known BBB markers (33).

ITM2A as an endothelial brain specific transmembrane protein has not been associated in the literature with brain transcytosis or transport. The present report describes the work we have done to characterize this target as a potential brain delivery candidate.

Materials And Methods

Animals

Male and Female Cynomolgus monkeys (Macaca fascicularis) aged from 4.8 to 5.9 years were purchased from Le Tamarinier and Noveprim Ltd. (Mahebourg, Mauritius). Six animals were group-housed in aviaries or interconnected mobile cages and two animals were individually housed in interconnected mobile cages. Animals were housed under controlled conditions (20–2 4°C, 40–70% humidity, 10–15 renewals per hour of filtered, non-recycled air, 12-h light cycle) with free access to filtered tap water and daily distribution of expanded diet (sodium dodecyl sulfate SDS, France) and fruits or vegetables. Animals used for the isolation of brain microvessels were at disposal following pre-clinical studies. Prior to the isolation of brain cortical microvessels, animals were submitted to a washout period of a minimum of 1 month.

Male mice C57BL6/J aged from 6 to 8 weeks were purchased from Charles River Laboratories (France)

Pregnant mice C57BL/6JRj were purchased from Janvier Lab's (France) between E10 and E12.

After arrival, mice were housed individually (for pregnant mice) or grouped (for male, 6 animals per cage) in an enriched environment in a pathogen-free facility at a constant temperature of 22 ± 2°C and humidity (50 ± 10%) on a 12-h light/dark cycle with ad libitum access to food and water.

Male rats Wistar: crl WI were purchased from Charles River Laboratories (Germany) After arrival, rats were housed individually in an enriched environment in a pathogen-free facility at a constant temperature of 22 ± 2°C and humidity (50 ± 10%) on a 12-h light/dark cycle with ad libitum access to food and water.

Isolation of Brain Microvessels from Cynomolgus Monkey and rodents Cortex

Brains from Cynomolgus monkeys or rodents were collected shortly after the euthanasia of the animal into ice-cold Hibernate A medium (ThermoFisher). All subsequent steps were performed at 4 °C and under a biological safety cabinet. Brain cortex was isolated and placed in petri dishes containing ice-cold Hanks' Balanced Salt solution HBSS. The meninges and the cortical white matter were removed. The collected tissues were transferred into a new sterile container with HBSS, finely minced with a scalpel, and then pelleted by centrifugation (5 min at 600 g, 4°C). The pellet was resuspended in a collagenase/dispase solution (Roche, Meylan, France, Collagenase 0.1 U/mL; Dispase 0.8 U/mL prepared in Ca2+/Mg2+ free HBSS) containing type I DNAse at 20 U/mL and Tosyl-L-lysyl-chloromethane hydrochloride (TLCK) at 0.147 g/mL, and incubated at 37°C for 60 min, under vigorous agitation. The digested tissue was carefully homogenized, and centrifuged for 5 min at 600 g, 4°C. The resultant pellet was resuspended in HBSS containing 20% Bovine serum albumin (BSA) and centrifuged at for 30 min at 2000 g, 4°C. The myelin ring-containing supernatants were discarded, and the vessel-containing pellet was resuspended and re-incubated in the collagenase/dispase solution in presence of DNAse and TLCK for 30 min at 37°C (except microvessels from mice). This suspension was re-pelleted by centrifugation 5 min at 600 g, 4°C, and the final pellet (named passage 0 Day in vitro 0 (P0D0) fraction from this point onwards) is resuspended in endothelial cell medium endothelial basal medium (EBM-2) supplemented with Kit endothelial cell growth medium micro vascular (EGM-2 MV) Single Quots, Lonza, Basel, Switzerland) containing 3 g/mL puromycin, before set up in pre-coated (collagen IV 100 g/mL, fibronectin 10 g/mL, Sigma, Saint Quentin Fallavier, France) cell culture flasks, and incubated at 37°C, 5% CO2 for 7 days. Every 2 days the cell medium was changed, the supplemented puromycin concentration lowered to 2 g/mL, and subsequently removed. Following 7 days of expansion at P0D7, Brain Endothelial Cell (BEC)s from cortex, were further singularized and re-plated de novo for further 7-day cell expansion (P1D7).

Stable cell lines generation

Plasmid constructs

Various human influenza hemagglutinin (HA) human ITM2A cDNA with coding sequence: NM_004867 and its variants were synthetically made by GeneART and introduced in a PiggyBac® transposon mammalian expression vector pBH 6450 with a Cytomegalo virus (CMV) promoter. HA tag is inserted at different position in ITM2A sequence: at NH2 or COOH side or in the Brichos domain: at NH2 or COOH side of the Brichos domain or in the middle in order to disrupt the eventual function of this domain. Plasmids were named: pBH-hITM2A HA NH2, pBH-hITM2A HA COOH, pBH-hITM2A wild type (wt), pBH-hITM2A Brichos HA COOH, pBH-hITM2A Brichos HA NH2, pBH-hITM2A4 Brichos HA mid.

Various Green Fluorescent Protein (GFP) ITM2A constructs with coding sequence: NM_004867 for human and NM_008409 for mouse were introduced in pcDNA6.2™C-Emerald (Em)GFP or pcDNA6.2™N-EmGFP expression vectors with CMV promoter and blasticidin resistance. GFP tag is inserted at different positions in mouse or human ITM2A sequences: at NH2 or COOH sides. Plasmids were named:

pcDNA6.2™N-EmGFP -hITM2A, pcDNA6.2™N-EmGFP -mITM2A, pcDNA6.2™C-EmGFP -hITM2A, pcDNA6.2™C-EmGFP -mITM2A.

Cells and cloning

HEK293/CVCL_0045 cells were obtained from Deutsche Sammlung von Mikroorganismen und Zellkulturen (DSMZ). For thawing: cells are thawed rapidly in water bath at 37°C, centrifuge at 900 g for 4mn, pellet is re-suspended in culture medium. Cells are cultured in the following medium: Dulbecco's Modified Eagle Medium Gibco 21969 (glutamine-free: selection pressure for HA tag or Blasticidin 15µg/mL: selection pressure for GFP tag); 10% Foetal Calf Serum Eurobio CVFSVF06 heat inactivated Australian; Penicillin / Streptomycin Gibco 15140 100 U / mL final. At confluence, the cells are rinsed with Phosphate-buffered saline (PBS) (-Ca2+, -Mg2+), detached by enzymatic treatment (Accutase Sigma A6964 or trypsin) at 37°C for 3mn, centrifuge at 900g for 4mn. The pellet is re-suspended in culture medium and diluted to 1/10 in fresh medium for seeding in new flasks.

Human Cerebral Microvascular Endothelial Cell (hCMEC)/D3 cells were obtained from Cedarlane. Cells are cultured in the medium cell biologics add with supplements for endothelial cells H1168 as described above.

HEK293/CVCL_0045 cells were transfected with pcDNA6.2™-*EmGFP* or cotransfected with PiggyBac® transposon expression vectors bearing wt *ITM2A* and variants cDNAs and transposase plasmids 6209 (10:1) by using Lipofectamine 2000®, following manufacturer instructions. Transfections were performed at 50% confluence in 24 wells plate with 500 ng of plasmids. For stable transfections, clones are obtained by limit dilution in 96 well plates with blasticidin selection for pcDNA 6.2 or in glutamine free media corresponding to the glutamine synthase selection marker of pBH 6450. Each individual cell is amplified in a 6 wells plate, then *ITM2A* expression is checked first with fluorescent microscope for GFP tag, second by Western Blot for all ITM2A constructions.

Antibody generation

Antigen preparation

The human and murine *ITM2A* extra-cellular domain (ECD) gene sequence was synthesized and fused to a human Fc in a mammalian expression vector. After preparation of transfection-grade DNA, a transient transfection of HEK293 cells was performed. After 7 days of cultivation, the ITM2A-Fc containing culture supernatant was isolated and purified by Protein A affinity chromatography according to standard protocols. After buffer exchange to PBS, the purified antigen was analyzed by UV/VIS spectrometry and SDS-PAGE.

Antibody-phage selection

The target protein (ITM2A-human Fc) and negative antigen (Protein N Standard, Siemens, QQIM13) were immobilized onto the wells of an Enzyme-Linked Immunosorbent Assay (ELISA) plate (Corning, 9018) for

1 h at room temperature (RT) (1 µg each). After removal of non-bound antigen, ELISA wells were blocked with a 2% BSA solution for 16 h at 4 °C. After washing of the plates with PBS-T (PBS containing 0.05% Tween 20), the antibody-phage library was added to the immobilized negative antigen and incubated for 1 h at RT to remove Fc specific or polyreactive antibody-phage. Additionally, 5 µg Protein N Standard was added as soluble competitor. Non-bound antibody-phage were recovered and incubated on the immobilized target antigen for 2 h at RT. Non-bound or weakly bound antibody-phage were removed by washing with PBS-T (10x) before antigen-specific phage were recovered by Trypsin (10 µg/ml) elution for 30 min at 37 °C. The antibody-phage were rescued by infection of TG1 cells (OD600=0.5) for 30 min at 37 °C. After propagation of the cells for additional 30 min at 37 °C and 500 rpm, ampicillin (100 µg/ml) and glucose (100 mM) were added to the 2YT culture medium. Bacterial propagation was continued for 1 h at 37 °C and 500 rpm. Then, bacteria were co-infected with M13K07 helper phage, incubated at 30 min at 37 °C followed by another incubation for 30 min, 37 °C and 500 rpm. Double-infected bacteria were centrifuged (4000 g, 10 min) and the cell pellet was resuspended in fresh 2YT, containing Ampicillin (100 µg/ml) and Kanamycin (50 µg/ml). For the amplification of antibody-phage particles, the incubation was continued for 16 h at 30 °C. Then, the culture was centrifuged (4000 g, 10 min) and antibody-phage containing supernatant was recovered and used for the next panning cycle. Three panning cycles were performed in total. In each cycle, the number of washing steps was increased (cycle 2: 20x, Cycle 3: 30x) to increase the stringency of the selection.

Antibody screening and sequence analysis

After the third panning cycle, the eluted phage were used to infect XL1 (OD600=0.5) for 30 min at 37 °C and streaked out on 2YT agar plates, containing ampicillin (100 µg/ml), glucose (100 mM) and tetracycline (20 µg/ml). Incubation was continued at 37 °C until single colonies were observed. Single clones were isolated and transferred into 96-well plates, containing 2YT, ampicillin (100 µg/ml), glucose (100 mM) and tetracycline (20 µg/ml). The bacteria were cultivated for 16 h at 37 °C and 300 rpm. Then, 15 µl of the overnight cultures were used to inoculate new 96-well plates, containing 2YT medium, ampicillin (100 µg/ml), tetracycline (20 µg/ml) and IPTG (50 µM). The bacteria were cultivated for 16 h at 30 °C and 300 rpm. The cultures were centrifuged (4000 g, 10 min) and Single-Chain Variable Fragment (scFv) containing supernatants recovered. The scFv containing supernatants were used for antibody screening. In brief, supernatants were diluted with a 2% BSA solution (in PBS, containing 0.05% Tween20), added to the immobilized antigens in a 384 well ELISA plate (20 ng/well) and incubated for 1 h at RT. After washing, binding of the scFv antibodies to human ITM2A-human Fc, murine ITM2A-human Fc, Protein N Standard or BSA was detected via a Myc-tag using a secondary horseradish Peroxidase (HRP) conjugated antibody. The binding was quantified by TMB reaction and absorbance reading at 450 nm. Target specific antibody clones were isolated, and the DNA sequence of the respective scFv antibody analyzed by sanger sequencing.

Immunoglobulin G (IgG) expression

The VH and VL sequence of selected antibody clones was amplified by PCR and cloned into mammalian IgG expression vectors. After preparation of transfection-grade DNA, a transient transfection of HEK293 cells was performed. After 7 days of cultivation, the IgG containing culture supernatant was isolated and purified by Protein A affinity chromatography according to standard protocols. After buffer exchange to PBS, purified antibodies were analyzed by UV/VIS spectrometry, SDS-PAGE and flow cytometry analysis for cell binding.

Transcriptomic

Transcriptome Sequencing (RNAseq) and mRNA Expression Analysis COMPACT IMI consortium

As described previously by Li et al (11).

RNA Samples for Library Preparation

As described previously by Chaves et al (34) Frozen cell pellets from the cellular P0D0, P0D7 and P1D7 fractions were lysed using QIAzol Lysis Reagent (Qiagen, #79306, Courtaboeuf, France). Total RNA was then isolated from the lysates on a QIAcube instrument (Qiagen) using the Rneasy Mini QIAcube kit (Qiagen, #74116) and following the manufacturer's instructions. The RNA concentration was determined using the Qubit RNA HS Assay Kit (Invitrogen, #Q32852, Illkirch-Graenstaden, France) and the quality and integrity was assessed on a Bioanalyzer 2100 (Agilent Technology, Les Ulis, France) with an Agilent RNA 6000 nano kit (Agilent Technology, #5067-1511).

RNA Sequencing (RNAseq)

As described previously by Chaves et al (34), the RNAseq libraries were prepared with 30 ng of input total RNA using the NEBNext Ultra II Directional RNA Library Prep Kit for Illumina (New England Biolabs, #E-7765S, Évry-Courcouronnes, France) with the NEBNext rRNA Depletion Kit (New England Biolabs, #E6310L) and following the manufacturer's instructions. The libraries were then paired end sequenced (75 cyclesx2) on the NovaSeq 6000 instrument (Illumina, Paris, France) using the NovaSeq 6000 SP Reagent Kit (300 cycles; #20027465, Illumina).

Reverse transcription quantitative Polymerase Chain Reaction (RTqPCR)

Cells or tissus were lysed with RLT buffer from Qiagen added with 1% β-mercapto-ethanol according to manufacturer instructions. mRNA was extracted with Qiagen MiniKit followed by DNase step using the Qiacube robot. Reverse Transcription is achieved from 250 ng of mRNA with High Capacity cDNA Reverse Transcription Kit from AppliedBiosystem Ref 4368813. qPCR is performed from cDNA diluted 1/20 using QuantStudio™ 7 in 384 wells with the TaqMan system standard mode and following manufacturer instructions. Primers and Probes Taqman were bought at thermoficher scientific inventoried assay ref 4331182, ITM2A: Mm00515208_m1; Actin: Mm01205647_g1; glyceraldehyde-3-phosphate deshydrogenase (GAPDH) Mm99999915_g1; Platelet endothelial cell adhesion molecule (PECAM) 1 Mm01242576_m1. Raw data were analyzed with QuantStudio™ Real-Time PCR software.

Proteomics

Immunocytochemistry

Cultured cells were fixed in 4% paraformaldehyde for 15 min, at RT, and subsequently permeabilized and blocked in Blocking Buffer Odyssey LiCor containing 0.2% Triton X-100. Primary antibodies were incubated overnight at 4°C (anti-ITM2A polyclonal AF4876 and 14407-1-AP, monoclonal non-commercial provider Yumab: YU93-G04, YU147-A01 YU147-E02 YU147-H07, anti-EmGFP A31852 or A11122, anti-HA 901509), and appropriate secondary antibodies conjugated with Alexa fluorophores (Invitrogen) and Hoechst 33432 (Invitrogen) for nuclei staining were subsequently used for 2h at RT. Images were acquired on a Perkin Elmer Operetta CLS system.

Colocalization confocal imaging

Confocal microscope images were acquired with SP8 LEICA microscope, 40X objectives. For the acquisition ITM2A was directly visualized by EmGFP 488. Organelles were stained with following primary antibodies anti Lysosomal-associated membrane protein 1 (LAMP1) ab24170 for lysosome detection, anti-giantin ab37266 for Golgi. Antibody anti-organelle were detected by staining with appropriate secondary antibody Alexa 633 goat anti mouse A21050 1/1000 or goat anti rabbit A21070 1/1000

Western Blot

NHP-derived BEC were lysed using ice-cold radio-immunoprecipitation assay (RIPA) or cell lysis buffer containing protease inhibitor cocktail (ThermoFisher) centrifuged at 15,000 g for 15 min, and supernatant fractions were collected. Samples were added with SDS and loading buffer then denaturized by heat 95°C for 5 min. These were loaded into 4–12% Tris-Glycine SDS-page gels (Invitrogen), and let to migrate for 1h at 180V. Samples were then transferred onto polyvinylidene fluoride (PVDF) or nitrocellulose membranes using an iBlot 2 Dry Blotting System (Invitrogen) on the P0 program (20 V for 1 min, 23 V for 4 min, 25 V for 2 min). PVDF membranes were then rinsed with Tris-buffered saline with 0.1% Tween 20 (TBST) and blocked for 1 h in 5% non-fat dry milk in TBST (blocking buffer). Membranes were first probed overnight at 4°C with primary antibodies in blocking buffer (anti-ITM2A polyclonal AF4876 and 18306-1-AP, EmGFP A11122, anti-HA 901509, anti α-tubulin T9026) and then probed with secondary antibodies diluted in TBST for 1 h at RT (1:10,000 diluted HRP-coupled goat anti-mouse IgG or goat anti-rabbit IgG, GEHealthcare). Following secondary antibody incubation, membranes were rinsed thoroughly with TBST, imaged using a LICOR Odyssey Imager and bands quantified using Multi-Gauge v3.0.

Mass spectrometry

Post-mortem human brain samples (occipital cortex, devoid of pathological findings) from three 69 to 79-year-old, male, non-demented, control donors were obtained from external biological resource centers in full accordance with legislation and ethical standards. Microvessels were isolated as described above for monkeys. Tissus or cells were lysed in Preomics 2X buffer then crushed gently with gentle MACS Dissociator Miltenyi Biotec, program Protein for 1min. Samples were centrifugated 10min at 4000g, 4°C,

supernatants were collected and dilute to 1X Preomics buffer. Benzonase 1/100 was added and incubated 10 min à 95°C, 1000 rpm. Samples were centrifugated 20mn at 13000g and supernatants were collected. Proteins are quantified by spectrophotometry using bicinchoninic acid method and spectraMax i3x. 25 µg of protein were digested on Preomics filter in 50µL following manufacturer instructions during 3h at 37°C, after evaporation, samples were diluted at 0,5µg/µL in 50µL LC-Load buffer, vortexed and sonicated. Heavy peptides were added to the sample solution to inject 5 fmol of heavy peptides and 2µg of proteins. 7 heavy stable isotope labelling (SIL) peptides spiked in final digest prior to Parallel Reaction Monitoring-Mass Spectrometry analysis on Q-Exactive HF /NanoRSLC 3500. From ITM2A_MOUSE Integral membrane protein 2A Q61500, spiked SIL peptides for detection were: IAFNTPTAVQK, NLVELFGK, EDLVAVEEIR, DLLLGFNK. Spiked SIL peptides used for hTFRC detection were: DSAQNSVIIVDK, LTVSNVLK, SGVGTALLLK, AAAEVAGQFVIK, LTTDFGNAEK.

Transport assays

Internalization assay

HEK293 ITM2A cells are cultured on 96 wells plate coated with poly-L-lysine at 50000 cells/well. After 24h cells were incubated 1h at 4°C in cell medium with 5µg/mL of studied antibody (Anti ITM2A RandDsystem AF4876, Yumab antibodies anti ITM2A YU147-A01, E02 and H07, YU93-G04, GFP antibodies A31852 or A11122, anti-HA 901509). Cells were washed with ice cold PBS then incubated 1h at 37°C or at 4°C for control. Cells were washed 2 times with ice cold PBS, then 2mn with acid buffer (glacial acid acetic 1/167 in PBS, pH = 2,5) and finally 2 times with ice cold PBS. Cells were fixed and stained as described above. Images were acquired with Operetta High Content Screening (PerkinElmer) objective 40X water confocal mode.

In Vitro Transcytosis and Permeability Measurements Brainplotting models

All human samples were provided by Brainplotting (35)(iPEPS, Institut du Cerveau et de la Moelle épinière, Hôpital Universitaire de la Pitié-Salpêtrière, Paris, France) in partnership with Sainte-Anne Hospital, Paris (neurosurgeon Dr. Johan Pallud) and harvested during tumor scheduled resection surgery with written informed consent from the patients (authorization number CODECOH DC-2014-2229). Human brain microvessels were obtained from surgical resections of one patient: a 35-years-old female suffering from of a diffuse oligoastrocytic grade III glioma. Microvessels were isolated from peritumoral or healthy brain tissue using an enzymatic procedure(34) adapting methods previously published for rats(36, 37). Briefly, tissue samples were carefully cleaned from meninges and excess of blood; then, an enzymatic mix was used to dissociate the tissues and microvessels were isolated by retention on a 10 mM mesh. Cells were cultured in EBM-2 medium (Lonza, Basel, Switzerland) supplemented with 20% serum and growth factors (Sigma)(36, 37). After seeding brain capillaries in petri dishes, brain primary microvascular endothelial cells were shortly amplified and seeded (P1D0) on Transwell (Corning) with microporous membranes (pore size: 0.4 mm) in monoculture.

Test (1 µg/mL of internal anti-human/cynomolgus Transferrin Receptor C (TFRC) antibody or anti-ITM2A YU93-G04) and control antibodies (1µg/mL mouse IgG, clone MG1-45, BioLegend) were added onto the upper chamber on day adapted to the transport assay defined by Brainplotting. Fresh endothelial cell medium with none of these compounds was added onto the bottom chamber. Final aliquots from both chambers were taken 240 min following incubation at 37°C, 5% CO2. Compound levels in mother solutions (T = 0 min), upper and lower compartments (T = 240 min) were determined by ELISA assay (MESOQuickPlex SQ120, MesoScale Discovery, Rockville, MD, USA). Apparent permeability (Papp) coefficients were calculated using the following formula:

Papp (cm/min) = (V /(A x Cluminal)) x (Cabluminal/ t)

where V = volume of cell medium in the bottom chamber (mL), A = surface area of the insert (cm^2), Cluminal = compound concentration loaded in the upper chamber (µM), Cabluminal = compound concentration measured in the bottom chamber (µM); t = time of the assay (min).

Immunoassay Method ELISA (in vitro and in vivo studies)

Standard 96-well sector plates (Meso Scale Discovery) were coated with 0.5 µg/mL of Fab'2 anti-Human (709-006-098 Jacksonimmuno) or anti-mouse (M0284 Sigma-aldrich) IgG in PBS and then incubated for 1 h under agitation at RT. After incubation, plates were washed three times with PBS-Tween 0.05% (Calbiochem, 524653) and blocked for 1 h at RT with 0.1% BSA solution (A7030, Sigma). After blocking the plates, collected samples in transport assay and standards were incubated on plates for 2 h at RT. After incubation, plates were washed three times with PBS-Tween 0.05%, and bound antibody was detected with SULFO-TAG conjugated goat anti-mouse antibody (R32AC-1, Meso Scale Discovery) or goat anti-human antibody (R32AJ-1, Meso Scale Discovery) using Tripropylamine containing read buffer (R92TC-2, Meso Scale Discovery). Concentrations were determined from the standard curve using a four-parameter non-linear regression program (Discovery Workbench version 4.0 software).

In vivo experimentations

Mouse brain collection

Each mouse was anaesthetized in isoflurane gas chamber then transcardiacally perfused with Li-heparinate solution at final concentration 20 U/mL in sterile PBS. Perfusion was realized with 48mL delivered at the speed of 8 mL/mn. Brain samples were collected. Each mouse was decapitated immediately after perfusion. Perfused brain was removed, cerebellum and brainstem were separated and eliminated. Brain cortex were washed in ice-cold PBS, collected in preweighted Precellys tube and stored immediately at -80°C freezer (or dry ice) until use. Then, the preweighted hemispheres were thawed and homogenized in 5 vol. (v/w) of brain lysis buffer (1% NP-40 in PBS containing complete mini ethylene diamine tetra-acetic acid - free protease inhibitor cocktail tablets, Pierce) using bead homogenizer. Homogenized brain samples were then rotated at 4°C for 1 hour before centrifuge at 20000 g for 20 min.

Pharmacokinetic study in vivo in mouse

5-10 mg/kg (35-70 nmol/kg) in a single dose of anti-ITM2A (clone YU93-G04) or control (anti- trinitrophenyl (TNP), batch VA2-17-419-1, internal production) antibodies were administrated by caudal intravenous injection into mice, C57Bl/6, male, 20-25g (n = 3/condition). 5h post-injection, plasma and saline-perfused brains were collected, then concentration was determined by ELISA immunoassay as described above

In vivo panning Yumab in mice

Yumab provided amplified phage library to Sanofi. First, a naïve human antibody phage library was enriched for antigen specific antibodies against ITM2A proteins. The antibody phage output was amplified and purified by poly-ethylene glycol (PEG)/ NaCl purification. Purified antibody phages were directly used for the in vivo panning: 1011 antibody phage particles (~10 µl) were mixed from each panning output. The antibody phage mix was injected into the mouse. Brains were isolated after 1 h and 24 h (2x each). Brains were collected as described above.

Antibody phages in the homogenate were used for infection of E. coli. Bacteria were selected and used for production of monoclonal scFv antibodies. About 800 clones were picked and screened by scFv in ELISA assay.

Statistical Analysis

The statistical significance of differences between groups was analyzed using GraphPad Prism v9.0.0 software (GraphPad Software, San Diego, CA, USA) Ordinary one-way Analysis of Variance (ANOVA) (non-parametric or mixed) with Dunnett's multiple comparisons test, Ordinary two-way ANOVA (mixed) with Sidak's, Kruskal Wallis or Mann-Whitney multiple comparison test or unpaired t test (non-parametric). The application of these statistical methods to specific experiments is noted in the Fig. legends.

Results

Our strategy is outlined in Fig. 2. The first objective was to produce tools to study the mechanisms: cells expressing ITM2A and the extracellular domain of the protein to produce antibodies preferably mouse-human cross reactive. With this in hand, uptake, internalization, and trafficking in either the above overexpressing cells or in BEC's would provide the first filter. Transcytosis and in vivo brain pharmacokinetic would lead to final validation (Fig. 2).

Building up cell lines expressing ITM2A

In the absence of available monoclonal antibodies, we devised a strategy that could bring clues on the potential of this protein to carry biologics into the brain using specific well characterized cargos. To this end, we engineered several constructs of human or murine *ITM2A*. One plasmid, named wt, was designed with no tag, the others bearing either an HA-tag (HA-tag are amino acids 98-106 of human influenza

hemagglutinin glycoprotein) or a GFP-tag at different positions, namely on the C-Terminal (C-Ter) extracellular domain or on the N-Terminal (N-Ter) intracellular domain of *ITM2A*. In addition, the HA tags were positioned at three distinct locations of the Brichos domain within the extracellular portion to bring additional insight on the potential position involved in internalization. This information could be exploited later for the generation of antibodies specifically recognizing a part of the antigen to optimize their transcytosis. Designed plasmids are summarized in Fig. 3.

We selected adherent HEK293 cells well suited for immunofluorescence analyses and produced 10 clonal cells lines by recombination with the various tagged or untagged mouse or human plasmids displayed in Fig. 3 (Table 1). Clones were obtained after limit dilution and selection by either fluorescence and Western Blot for GFP tag or by Western Blot for HA tag and wt *ITM2A* (Additional file 1).

Table 1
Engineered HEK293 cells expressing various tagged or untagged human or mouse ITM2A

Mouse *itm2a*		**Human *ITM2A***	
GFP tag	HA tag	GFP tag	No tag
N-Ter	N-Ter	N-Ter	wt
C-Ter	C-Ter	C-Ter	
	Brichos 1 C-Ter		
	Brichos 2 N-Ter		
	Brichos 3 Mid		
Several constructs of human or murine *ITM2A* with or without tags as GFP or HA			

Fluorescence ITM2A visualization

After cell line validation for the ITM2A construct protein expression by Western Blot (WB), cellular localization of both human and mouse ITM2A was visualized by fluorescence microscopy in cell lines using GFP fluorescence (Fig. 4). GFP fluorescence was detected in all N-Ter and C-Ter constructs in HEK293 expressing both human and mouse ITM2A.

Cellular localization of ITM2A

Aside from membrane localization as could be showed by the above binding experiments, ITM2A could be localized in Golgi of the overexpressing HEK293 cells after evidencing co-localization with Giantin (Fig. 5A). No ITM2A could be seen in the lysosomes as shown by LAMP1 co-labeling (Fig. 5B).

Cell uptake of antibodies

With these cell lines in hand, we went on to evaluate their capacity to uptake antibodies after binding with the protein. We could perform these experiments using several handles.

First, we performed immunofluorescence studies on HEK293 cells expressing human ITM2A with two commercially available polyclonal antibodies against extracellular epitopes of human ITM2A: AF4876 and 14407-1-AP (Fig. 6A and B). The first one displayed membrane labeling at 4°C while the second one could not be detected at 4°C maybe linked to a lower affinity or different behavior after acid washing (performed before analysis). Both antibodies readily internalized at 37°C leading to punctate labelling and demonstrating active uptake. The weaker signal observed with AF4876 on the C-Ter GFP cell line could result from steric hindrance of the GFP tag for antibody binding.

The same results were obtained using anti-GFP antibodies either directly fluorescent (A31852, Fig. 6C), or after detection of an unlabeled anti-EmGFP antibody (A11122) with a secondary labeled Alexa 647 anti-Fc rabbit antibody (Fig. 6D). In both cases, very clear membrane labeling could be observed at 4°C followed by internalization at 37°C with the HEK293 cells expressing human and murine C-Ter GFP ITM2A, but not N-Ter GFP ITM2A confirming the need for the GFP to be extracellular for recognition.

We generated analogous results with anti HA antibodies on HEK293 cells (Fig. 6E) where clear internalization could be observed when the label was in C-Ter leading to punctate labelling confirming that ITM2A was functional and able to internalize cargos such as antibodies into cells.

Similar results were obtained with anti GFP antibodies and mouse ITM2A GFP constructs in HEK293 cells expressing mouse ITM2A with C-Ter and N-Ter GFP demonstrating functional internalization of mouse ITM2A too (Fig. 7):

Production of monoclonal ITM2A antibodies

A campaign was launched in collaboration with Yumab and the COMPACT IMI consortium to generate mouse/human cross-reactive monoclonal antibodies. The genes of the murine and human ITM2A ECD were synthesized and fused to the human IgG1 Fc part on a mammalian antigen expression vector. After transient transfection of HEK293 cells, the ITM2A-Fc fusion proteins were expressed, secreted by the cells into the culture medium and purified. A total of four different antibody selections were performed using two antibody libraries consisting of human kappa or lambda antibodies, comprising together a diversity of more than 10^{10} different antibody sequences.

From 2304 clones tested for binding activity on the murine and human ITM2A, 220 cross-reactive and 15 mouse specific hits were identified. 19 cross reactive antibodies with unique sequences were selected, produced and purified as fully human IgG in HEK293 cells. Testing these antibodies on human ITM2A overexpressing HEK293 cells revealed low correlation between binding to the recombinant protein and cell binding. 4 IgG antibodies did exhibit potent cell binding. These antibodies could demonstrate binding and internalization analogously as shown previously. For instance, when HEK293 cells expressing wt, C-Ter or N-Ter GFP-ITM2A were exposed to G04, internalization occurred readily at 37°C (Fig. 8A).

Similarly Yumab A01, E02 et H07 and the control AF4876 displayed binding at 4°C with the cells. Upon washing and warming to 37°C they were internalized as evidenced by a punctiform labeling inside cells (Fig. 8B).

ITM2A expression in BEC's

With antibodies demonstrating binding and uptake in hand, our next step was to evaluate their capacity to perform transcytosis. Before we went on to evaluate our ITM2A antibodies in models of transcytosis we checked whether we could find ITM2A expression in our BEC's.

First, we checked *ITM2A* mRNA level in brain endothelial primary cells and cell lines. RNA levels were rapidly lost upon culture of non-human primate brain endothelial cells (Fig. 9A, cortex shown). Similar downregulation after culture was also observed in mouse primary BEC's (Fig. 9B). In comparison, cluster of differentiation 31's (CD31) expression, a specific marker of endothelial cells retained high expression throughout the culture. This downregulation most certainly also explains why no expression of *itm2a* could be found in bEnd.3 cell lines (Fig. 9B).

Likewise, we could not detect endogenous ITM2A protein in primary endothelial cells from brain cortex of mouse or rats by immunolabelling compared to mouse ITM2A overexpressing HEK293 cells which displayed nice immunolabeling with anti-mouse ITM2A antibodies (AF4876, 18306-1-AP and Yumab G04). (Fig. 10)

Similarly, we could not detect endogenous ITM2A protein in hCMEC/D3 by immunolabelling compared to TFRC probably due to the downregulation of ITM2A in culture (Fig. 11)

As immunolabelling showed no signal for ITM2A, we checked the level of ITM2A by WB using commercially available polyclonal antibody AF4876 and as a control we evaluated the mouse ITM2A-GFP fusion in HEK293 cells using an anti GFP antibody. The protein was well detected at the expected molecular weight (MW) (30 kDa for ITM2A+ 27 kDa for GFP) in the HEK293 overexpressing cells but could not be detected in mouse, rat or monkey primary endothelial cells or astrocytes nor could it be detected in other cell lines (bEnd.3, Madin-Darby Canine Kidney (MDCK1), hCMEC/D3) (Fig. 12).

We checked mRNA expression at several mice ages but could not see any marked difference. Decent expression (*itm2a* Cycle Threshold (Ct) = 25 vs *gapdh* Ct = 21) could be counted throughout post birth (P1) to six weeks of age in the cortex of mice (Fig. 13).

However, when these brain fractions were analyzed by WB, no band at 30 kDa could be identified (Fig. 14).

Proteomic studies to quantify ITM2A

To clarify whether ITM2A protein was or not present in the mouse, proteomic studies were engaged in mouse cortex and muscle of newborn (P1 and P2 stage) and adult mice, along with freshly prepared

astrocytes and brain microvessels in comparison with HEK293 cells overexpressing ITM2A. By Liquid Chromatography/ Mass Spectrometry (LC/MS), six endogenous peptides belonging to C-Ter or N-Ter ITM2A were used for detection and quantification. The results are shown in Fig. 15. While ITM2A was well detected in newborn muscle samples and in brain microvessels, less ITM2A was detected in both newborn and adult cortex samples and in adult muscle sample and no ITM2A was detected in astrocytes.

Protein intensities were calculated by averaging peptides intensity values (Fig. 15). After quantification of ITM2A in each sample, it could be calculated that the newborn cortex and muscle, brain microvessels and HEK293 cells overexpressing mITM2A averaged 0,1; 1,7; 0,6 and 3,6 fmol of ITM2A per µg of total protein content respectively.

From these experiments, it was concluded that ITM2A could be quantified in mouse brain and muscle albeit to a much lower extent in adult muscle and in cortex from newborn and adult. The protein was higher in brain microvessels freshly isolated from adult wt mice than in cortex homogenate pointing to endothelial cell enrichment. Levels of TFRC in mouse brain microvessels were quantified and found around the same range (0.8 fmol/µg).

These results suggest that WB conditions might not have been sensitive enough to detect the levels of ITM2A present. This was verified by diluting HEK293 cell lysate overexpressing mouse ITM2A. From the above-determined levels of 3.6 fmol ITM2A/µg of protein we determined that our limit of detection using Western blotting (additional file 4) was 7.2 fmol of ITM2A, over 10-fold the levels found in brain microvessels.

Finally, ITM2A was quantified in human microvessels and found to be four times lower than TFRC (ITM2A 0.11 fmol/µg of total protein vs TFRC 0.4 fmol/µg of total protein which could suggest lower transcytosis efficacy (Fig. 16).

In vitro transcytosis in human primary BBB model

As the ITM2A protein could be quantified, we decided to study one of our anti-ITM2A antibodies in a transcytosis model. Because of the strong ITM2A downregulation upon culture, cell line derived models were excluded. Even primary models which require a minimal culture to access enough endothelial cells were ruled out as we showed that in our NHP primary model ITM2A was already strongly downregulated. Preparation of human primary endothelial cells suitable for transcytosis was difficult owing to the hurdle of obtaining very fresh post-mortem human brains. We decided to turn to a human primary BEC model prepared from freshly resected brain tissue from glioblastoma or epilepsy surgeries provided by Brainplotting.

Anti ITM2A YU93-G04 antibody was evaluated in the model. As seen on Fig. 17A, the antibody did not perform better than a control antibody. In this model, an anti-TFRC receptor antibody performed systematically better than the control antibody (Fig. 17B).

In vivo mouse brain exposure of ITM2A antibodies

To finally conclude on the potential of this protein to enhance brain exposure of antibodies, two in vivo mouse experiments were conducted.

A single administration study in mice of the anti ITM2A monoclonal antibody (mAb) G04 vs a control anti-TNP mAb was performed and levels of the mAbs in brain and plasma after 5h were determined. The mice were perfused with PBS before brain collection. The level of the antibodies was quantified using an ELISA assay. There was a weak (>= 2-fold) increase in brain exposure of the anti-ITM2A mAb compared to the anti-TNP (control) antibody (Fig. 18).

In a second experiment, a naïve human antibody-phage library was enriched for antigen specific antibodies against ITM2A. The antibody-phage output was amplified and purified by PEG/N antibody purification. The purified phage display library of >6 million phages (panning campaign PC084, Strategy S1-1-10, panning rounds 3, diversity 6.3 10E6, titer ~1.10E13 cfu/ml) anti ITM2A ScFv's was used for in vivo panning and injected in mice. Brain were isolated after 1h and 24h and the brain homogenates were used to perform infection of *E.coli*. Picking of ~800 clones, screening of scFv supernatant in ELISA and on cells did not allow to identify any ITM2A phages in the brain.

Discussion

Endothelial cells form biological barriers that regulate exchanges and maintain a low and selective permeability to fluid and solutes under normal physiological conditions. Understanding their specific or enriched membrane proteins has been critical to facilitate drug delivery to specific organs. Within these organs, brain is indeed the most highly protected tissue. The blood brain barrier with its network of tight junctions, efflux pumps and specific metabolic systems represents a huge challenge for xenobiotics, drugs and especially large and polar biomolecules(1, 2). Several strategies are actively pursued to enhance brain exposure of biotherapeutics, one the most successful is certainly making use of an endogenous transcytotic receptor located on the BBB such as transferrin or insulin receptor(4). However, the mechanisms so far identified for brain enhancement have been mostly ubiquitously expressed leading to exposure in other tissues than brain which could potentially lead to pleiotropic and adverse effects. Identification of brain-specific mechanisms remains the ultimate unreached goal and is the active focus of current research in this area.

Two main workflows have been reported for the search of new mechanisms of brain delivery: On one hand transcriptomic and proteomic approaches from either brain microvessels or endothelials cells of human(38), cynomolgus monkey(39), bovine(40), rat(31, 41) or mouse(12, 42–45), including human(32, 46–48) diseased brains. On the other hand, phenotypic in vitro or in vivo screening of antibody's and peptide libraries displayed in various formats including phage and yeast(49–51). Only a few of them have delivered new brain delivery targets. Proteomics of rodent BEC's have led to CD98 heavy chain (a solute carrier) and Basigin (a matrix metalloprotease) along with known Lrp1 and InsR. Phenotypic panning of naïve lama single-domain antibody phage display for binding and internalizing in primary human BEC versus primary human lung endothelial cells led to FC5 and FC44(50). It was later shown that

FC5 binds to Cdc50A (energy-dependent clathrin endocytosis)(52). Our approach is combining both strategies.

Using proteomic, MicroArray and RNA sequencing approaches, the COMPACT IMI consortium identified candidate genes with high enrichment for brain, liver or lung of human primary endothelial cells(53). These identified proteins could have potential in understanding biological differences among these barriers and developing drugs to target specific organ. Analysis of the Next Generation Sequencing (NGS) data from human brain, liver and lung endothelial cells, selection of the genes with the highest expression in brain, differential expression versus peripheral tissues, annotation of human tissue, cell type and membrane localization using several public databases, led to few genes, some of them previously reported as brain delivery receptors such as LRP8(54) or Basigin(12) (54). Among them, ITM2A stood out with the highest differential expression. This protein has been reported as brain endothelial specific and identified from other omics efforts on rat(31) (32) and pig(33) BEC's. However, the function of this protein remains largely unknown, and it was never reported as a brain transporter.

To validate a putative transport mechanism for ITM2A along with potential for delivering drugs to the brain, we first developed cells overexpressing the protein with the aim to validate the protein membrane localization and look at binding and uptake of anti-ITM2A antibodies. At the start of this effort, we did not have access to monoclonal anti-ITM2A antibodies. Several anti-ITM2A antibodies were reported(15, 27) or commercially available but mostly polyclonal. We reasoned that engineering the protein with GFP and HA tags C-Ter (extracellular domain) position of the protein, could serve the double purpose of visualizing its cellular location using GFP fluorescence and allow the study of binding and uptake with antibodies against these tags. This strategy of tagging a protein to circumvent the absence of monoclonal antibodies has actually been reported for ITM2A for deciphering its role in hedgehog signalling pathway (55). Tags at the N-Ter were also engineered as controls along with several positions within the extracellular Brichos domain which could later bring information on the precise site for endocytosis. Exposure of the cells to anti-GFP antibodies first allowed to confirm ITM2A membrane localization. Cellular localization of ITM2A has been looked at in a few cell systems and shown on the plasmic membrane along with large cytoplasmic vesicles, possibly endosomes and the Golgi apparatus (15). In particular, cytosolic localization has been reported in HEK293 cells overexpressing ITM2A and that the protein could be found colocalized with LAMP1 in lysosomes (27). We have confirmed the presence of ITM2A in Golgi but not in lysosomes by colocalization experiments using GFP tags. In addition to binding, HEK293 cells demonstrated nice uptake of anti GFP or HA antibodies respectively. These binding and uptake were specific of cells overexpressing ITM2A bearing extracellular tags. The cells overexpressing ITM2A bearing intracellular tags did not lead to binding or uptake with these antibodies confirming that this uptake was specifically linked to extracellular binding to ITM2A. Internalization of receptors genetically engineered with extracellular tags such as HA, cMyc, EGFP, have been documented in the literature with some G-coupled receptors (56), Transforming Growth Factor β(57) or erythropoietin(58) receptors. However, this uptake is far from systematic and many antibodies do not internalize upon binding their antigen receptors as was shown for instance by Jacobsen et al with an anti-Myc antibody and myc-engineered GPR6 and β2-adrenergic receptors(59). The specific uptake of

these antibodies upon binding to the extracellular part of the protein was interpreted as a positive signal and gave us the second go for our validation flowchart. Monoclonal anti ITM2A antibodies were later designed and generated using the extracellular domain of ITM2A as antigen and the resulting antibodies confirmed the uptake seen previously.

Our next objective was to demonstrate that this uptake could lead to transcytosis in endothelial polarized cells. For this we needed a transcytosis model expressing the protein. It could be rodent or human as our anti ITM2A antibodies were cross reactive. From the COMPACT IMI consortium studies, it had been shown that the protein could no longer be found after an additional cell passage. We showed that ITM2A expression is strongly downregulated upon culture of either non-human primate(34) or mouse primary BEC's (Fig. 9) as is the case for several BBB genes after cell line establishment or culture (60, 61) and has already been shown specifically with ITM2A(33).

Most expression studies reported in the literature about ITM2A are transcript-based. In human, a good amount of the *ITM2A* transcript can be found in the brain as detailed in databases such as Gtex, Stanford, GenCard or open target platform (Fig. 1). In addition, according to Zhang et al, in humans, the amount of *ITM2A* mRNA in endothelial cells was evaluated at 150 Fragments Per Kilobase Million (FPKM) versus 23 FPKM for *TFRC* a well-known transcytotic receptor while in total brain the two proteins accounted for 2 FPKM. In mice, the amount of *ITM2A* mRNA was evaluated at 2000 FPKM in endothelial cells against 800 FPKM for *TFRC* and respectively 80 and 60 FPKM in the total brain for the two proteins (28).

Our own RNA seq study in non-human primate brain microvessels had shown intermediate expression of *ITM2A* in cortex, hippocampus and septum (FPKM 9-16) while very low expression in liver(34). By comparison in the same study, *TFRC* had shown a high expression (FPKM 75-125) in brain structures (34). Mitsui(25) reported that ITM2A protein was strongly detected in the lysates of mouse cerebral cortex between P0 and P10, and gradually decreased towards adulthood. Our own experiments on mice from P0 to 6 weeks of age showed that their *ITM2A* mRNA content remains constant throughout age. However, ITM2A protein could not be detected by WB in any of the samples, nor could it be detected in mouse, rat or monkey primary endothelial cells or astrocytes or in other cell lines (bEnd.3, MDCK1, hCMEC/D3) as opposed to the HEK293 cells overexpressing ITM2A where a strong band could be seen (Fig. 12). The theoretical MW of ITM2A is of ~30 kDa (Gencards or Proteintech) and it was reported that post translational modifications lead to an apparent MW of 43 and 45 kDa probably resulting from N-glycosylation at amino acid position 166 (15). Nevertheless, no protein could be detected around this MW either. Fluorescence gave the same results with strong signal for the HEK293 cells and no signal for endothelial rat or mouse cells or hCMEC/D3 cells confirming results from Masuda et al(62).

Using more sensitive proteomics, we were able to quantitate levels of ITM2A in mouse brain microvessels. These levels have been confirmed to be under the limit of detection of our WB conditions. Nevertheless, as these levels were in the same range as the ones found for TFRC in the same study, we considered that it was worth engaging into a transcytosis experiment.

We decided to evaluate one of our monoclonal anti ITM2A antibody in a model based on primary cultures of human BMEC from Brainplotting(35). These cells are prepared from fresh brains derived from surgical resections after very short time culture which gives them a better chance to keep their phenotype. In this model, a TFRC antibody reproducibly shows enhanced apparent permeability vs a control antibody. However, when the ITM2A antibody was evaluated in the same conditions, no difference in permeability vs the control could be evidenced (Papp ITM2A 0,97.10-6 vs control 1,02.10^{-6} cm.min-1). As we had no information regarding the status of ITM2A levels in this model, we could not clearly conclude on this experiment.

The area of predictivity of in vitro blood brain barrier models is still the matter of intense research and debate. Even if some antibodies brain exposures have been linked to their apparent permeabilities in in vitro transcytosis models(63, 64), this was shown in cases where in vitro and in vivo experiments were performed in the same species as described by Stanimirovic et al in rat(63). In vivo brain exposure, distribution and pharmacokinetics are dependent on a series of dynamic processes, linked also to target engagement, localization and cellular trafficking. All these would be difficult to recapitulate in an in vitro model even more so for species-to-species predictions where additional parameters such as anatomy, capillary bed density, molecular composition, as well as the density of specific BBB transporters(63) need to be taken into account.

To conclude about the potential of ITM2A to transport antibodies to the brain, we engaged one of our specific anti ITM2A antibodies directly in vivo in mice to quantify its brain exposure. When injected at 5 mg/Kg YU93-G04 could be quantitated in brain parenchyma 5h after injection with a 2-fold higher level than a control antibody. The brain/plasma ratio were not very different though for ITM2A and control antibodies (around 0.3%). This ratio was in the range of what is described in the literature regarding brain /plasma ratio for antibodies with no modification to enter the brain : 0.1% in the rat(65, 66) and 0.01% in primates(65–67) .To further evaluate if this modest brain exposure increase observed was mechanism-related and monitor an early time after injection (1h), we performed in vivo panning of a library of anti ITM2A antibodies. A naïve human antibody-phage library was enriched for ITM2A specific antibodies against recombinant protein ITM2A and the antibody-phage output was amplified and purified by PEG/NaCl purifications before injection to a single mouse. The brain was harvested at 1 and 24h after injection and the homogenates were used for infection of E. coli. From this no hit was identified suggesting that none of them was able to specifically reach the brain parenchyma. Phages are huge entities, and their barrier crossing might be more difficult than isolated antibodies. In addition, our anti ITM2A antibody could be trapped in the vessels or recycling(68). Alternatively, the epitope recognized by the antibody we selected for in vivo study might not be the one leading to transcytosis. To finally conclude about the fate of ITM2A antibodies after in vivo injection and their potential to enhance brain exposure, several antibodies recognizing distinct epitopes should be compared, and the antibodies quantitated in both parenchyma and vessels. At this stage, we considered that the enhancement obtained was not at the level that could be of interest for potential application to a therapeutic project.

Conclusions

Our work combines both transcriptomic profiling leading to selection of ITM2A as a potential brain specific target, and in vivo phage panning of an anti ITM2A phage library. Our approach illustrates the complexity of such endeavor. Not even mentioning the technical challenge of getting access to pure human primary endothelial cells, highly expressed targets are often down regulated upon culture making it difficult to study them in functional cellular models, cross-reactive monoclonal antibodies are necessary for validation in rodent models. In addition, targets might have different function in rodent and human although we have no indication that this could be the case for ITM2A. ITM2A might remain a valid target for human brain enhancement but its validation might prove quite complex.

Abbreviations

ANOVA: Analysis of Variance

BBB: Blood Brain Barrier

BEC: Brain Endothelial Cell

BMEC: Brain Microvascular Endothelial Cells

BSA: Bovine Serum Albumin

CD: Cluster of Differentiation

CMV: CytoMegaloVirus

CNS: Central Nervous System

COMPACT: Collaboration on the Optimization of Macromolecular Pharmaceutical

Ct: Cycle Treshold

C-Ter: C-Terminal

EBM: Endothelial Basal Medium

ECD: ExtraCellular Domain

ELISA: Enzyme-Linked Immunosorbent Assay

Em: Emerald

FPKM: Fragments Per Kilobase Million

GAPDH: GlycerAldehyde-3-Phosphate DesHydrogenase

GFP: Green Fluorescent Protein

HA: HemAgglutinin

HBSS: Hanks' Balanced Salt Solution

hCMEC/D3: Human Cerebral Microvascular Endothelial Cell

HEK293: Human Embryonic Kidney

HRP: horseradish Peroxidase

ICD: IntraCellular Domain

IgG: Immunoglobulin G

IMI: Innovative Medicines Initiative

ITM2A: InTegral Membrane protein 2A

LAMP1: Lysosomal-Associated Membrane Protein 1

LC/MS: Liquid Chromatography/ Mass Spectrometry

LRP8: Low-density lipoprotein Receptor-related Protein 8

mAb: monoclonal Antibody

MDCK: Madin-Darby Canine Kidney

MW: molecular weight

NGS: Next Generation Sequencing

NHP: Non-Human Primate

N-Ter: N-Terminal

P0D0: Passage 0 Day in vitro 0

P1: Post-birth 1

Papp: Apparent permeability

PBS: Phosphate-Buffered Saline

PEG: Poly-Ethylene Glycol

PVDF: PolyVinyliDene Fluoride

RIPA: Radio-ImmunoPrecipitation Assay

RT : Room Temperature

RTqPCR : Reverse Transcription Quantitative Polymerase Chain Reaction

scFv: Single-Chain Variable Fragment

SDS: Sodium Dodecyl Sulfate

SIL: Stable Isotope Labelling

TBST: Tween Tris-Buffered Saline

TFRC: Transferrin Receptor C

TLCK: Tosyl-L-lysyl-Chloromethane Hydrochloride

TM: TransMembrane domain

TNP: TriNitroPhenyl

WB: Western Blot

Wt: Wild Type

Declarations

Ethics declarations

Experiments were performed at Sanofi in our Association for Assessment and Accreditation of Laboratory Animal Care (AAALAC)-accredited facility in full compliance with standards for the care and use of laboratory animals, according to the French and European Community (Directive 2010/63/EU) legislation. All procedures were approved by the local animal ethics committee (Ethical Committee on Animal Experimentation [CEEA] #24 and #21), of Sanofi, Vitry-Alfortville and Chilly Mazarin Research Centers, France, and the French Ministry for Research.

Consent for publication

Not applicable.

Availability of data and materials

All data generated or analysed during this study are included in this published article and its supplementary information files.

Competing interests

The authors declare that they have no competing interests.

Funding

Funding for the present work was supported by Sanofi and COMPACT IMI consortium.

Author's Contributions

CC, CCH, TMD, VR and DL were involved in the design, analysis, and interpretation of data and manuscript writing. CD and JCG performed the mass spectrometry analysis. BD generated tagged plasmids. AF and PK performed ITM2A monoclonal antibodies production and phage display study. All authors participated in the critical editing of the manuscript. All authors read and approved the final manuscript.

Acknowledgements

We are grateful to Axel Meyer for his strong involvement in the COMPACT IMI consortium data analyses and his active reading of the manuscript. We are thankful to Martin Lenter, Klaus Fuchs and Simon Plythe for bringing Yumab to the project and active reading of the manuscript. We warmly thank Anne-Céline Le-Fevre for colocalization images, Corinne Célinain for mass spectrometry experiments and Patricia Senneville for the copyright requests.

Author informations

Affiliations

[1]Sanofi, Rare and Neurologic Diseases Research Therapeutic Area, Sanofi, Chilly Mazarin, France; [2]Sanofi, Proteomics, Translational Science, Sanofi, Chilly Mazarin, France; [3]Sanofi Biological Research, Sanofi, Vitry-Sur-Seine, France; [4] Yumab GmbH, Braunschweig, Germany

Corresponding authors

Correspondence to Céline Cegarra.

References

1. Banks WA. From blood-brain barrier to blood-brain interface: new opportunities for CNS drug delivery. Nat Rev Drug Discov. 2016;15(4):275-92.

2. Obermeier B, Daneman R, Ransohoff RM. Development, maintenance and disruption of the blood-brain barrier. Nat Med. 2013;19(12):1584-96.
3. Kumar NN, Pizzo ME, Nehra G, Wilken-Resman B, Boroumand S, Thorne RG. Passive Immunotherapies for Central Nervous System Disorders: Current Delivery Challenges and New Approaches. Bioconjug Chem. 2018;29(12):3937-66.
4. Lesuisse D. Increasing brain exposure of antibodies BBB Book. 2020.
5. Boado RJ, Hui EK, Lu JZ, Pardridge WM. Glycemic control and chronic dosing of rhesus monkeys with a fusion protein of iduronidase and a monoclonal antibody against the human insulin receptor. Drug Metab Dispos. 2012;40(10):2021-5.
6. Johnsen KB, Burkhart A, Thomsen LB, Andresen TL, Moos T. Targeting the transferrin receptor for brain drug delivery. Prog Neurobiol. 2019;181:101665.
7. Demeule M, Regina A, Che C, Poirier J, Nguyen T, Gabathuler R, et al. Identification and design of peptides as a new drug delivery system for the brain. J Pharmacol Exp Ther. 2008;324(3):1064-72.
8. Gabathuler R. Development of new peptide vectors for the transport of therapeutic across the blood-brain barrier. Ther Deliv. 2010;1(4):571-86.
9. Molino Y, David M, Varini K, Jabes F, Gaudin N, Fortoul A, et al. Use of LDL receptor-targeting peptide vectors for in vitro and in vivo cargo transport across the blood-brain barrier. FASEB J. 2017;31(5):1807-27.
10. Stanimirovic DB, Sandhu JK, Costain WJ. Emerging Technologies for Delivery of Biotherapeutics and Gene Therapy Across the Blood-Brain Barrier. BioDrugs. 2018;32(6):547-59.
11. J.Li AM, I.Mäger, H.J. Johansson, M.Lenter, T. Hildebrandt, G.Leparc, C.Untucht, J.Sim, M.Gumbleton, S.Plyte, W.Zhang, T.Letoha, S.El Andaloussi, R.Bell, D.Lesuisse, M.J. A. Wood. Proteomic and transcriptomic study to identify membrane proteins highly enriched in brain, lung and liver microvascular endothelial cells using human primary cultures. Scientific reports, manuscript in preparation.
12. Zuchero YJ, Chen X, Bien-Ly N, Bumbaca D, Tong RK, Gao X, et al. Discovery of Novel Blood-Brain Barrier Targets to Enhance Brain Uptake of Therapeutic Antibodies. Neuron. 2016;89(1):70-82.
13. R. Watts YJ, M. Dennis, P.-O. Freskgard. WO2011/091304A1. 2011.
14. Deleersnijder W, Hong G, Cortvrindt R, Poirier C, Tylzanowski P, Pittois K, et al. Isolation of markers for chondro-osteogenic differentiation using cDNA library subtraction. Molecular cloning and characterization of a gene belonging to a novel multigene family of integral membrane proteins. J Biol Chem. 1996;271(32):19475-82.
15. Kirchner J, Bevan MJ. ITM2A is induced during thymocyte selection and T cell activation and causes downregulation of CD8 when overexpressed in CD4(+)CD8(+) double positive thymocytes. J Exp Med. 1999;190(2):217-28.
16. Lagha M, Mayeuf-Louchart A, Chang T, Montarras D, Rocancourt D, Zalc A, et al. Itm2a is a Pax3 target gene, expressed at sites of skeletal muscle formation in vivo. PLoS One. 2013;8(5):e63143.

17. Van den Plas D, Merregaert J. Constitutive overexpression of the integral membrane protein Itm2A enhances myogenic differentiation of C2C12 cells. Cell Biol Int. 2004;28(3):199-207.
18. Boeuf S, Borger M, Hennig T, Winter A, Kasten P, Richter W. Enhanced ITM2A expression inhibits chondrogenic differentiation of mesenchymal stem cells. Differentiation. 2009;78(2-3):108-15.
19. Pittois K, Wauters J, Bossuyt P, Deleersnijder W, Merregaert J. Genomic organization and chromosomal localization of the Itm2a gene. Mamm Genome. 1999;10(1):54-6.
20. Richter GH, Fasan A, Hauer K, Grunewald TG, Berns C, Rossler S, et al. G-Protein coupled receptor 64 promotes invasiveness and metastasis in Ewing sarcomas through PGF and MMP1. J Pathol. 2013;230(1):70-81.
21. Tuckermann JP, Pittois K, Partridge NC, Merregaert J, Angel P. Collagenase-3 (MMP-13) and integral membrane protein 2a (Itm2a) are marker genes of chondrogenic/osteoblastic cells in bone formation: sequential temporal, and spatial expression of Itm2a, alkaline phosphatase, MMP-13, and osteocalcin in the mouse. J Bone Miner Res. 2000;15(7):1257-65.
22. Van den Plas D, Merregaert J. In vitro studies on Itm2a reveal its involvement in early stages of the chondrogenic differentiation pathway. Biol Cell. 2004;96(6):463-70.
23. Kihara M, Kiyoshima T, Nagata K, Wada H, Fujiwara H, Hasegawa K, et al. Itm2a expression in the developing mouse first lower molar, and the subcellular localization of Itm2a in mouse dental epithelial cells. PLoS One. 2014;9(7):e103928.
24. Liu GY, Ge CR, Zhang X, Gao SZ. Isolation, sequence identification and tissue expression distribution of three novel porcine genes--RAB14, S35A3 and ITM2A. Mol Biol Rep. 2008;35(2):201-6.
25. Mitsui S, Osako Y, Yuri K. Mental retardation-related protease, motopsin (prss12), binds to the BRICHOS domain of the integral membrane protein 2a. Cell Biol Int. 2014;38(1):117-23.
26. Biverstal H, Kumar R, Schellhaus AK, Sarr M, Dantuma NP, Abelein A, et al. Functionalization of amyloid fibrils via the Bri2 BRICHOS domain. Sci Rep. 2020;10(1):21765.
27. Namkoong S, Lee KI, Lee JI, Park R, Lee EJ, Jang IS, et al. The integral membrane protein ITM2A, a transcriptional target of PKA-CREB, regulates autophagic flux via interaction with the vacuolar ATPase. Autophagy. 2015;11(5):756-68.
28. Zhang Y, Sloan SA, Clarke LE, Caneda C, Plaza CA, Blumenthal PD, et al. Purification and Characterization of Progenitor and Mature Human Astrocytes Reveals Transcriptional and Functional Differences with Mouse. Neuron. 2016;89(1):37-53.
29. McKenzie AT, Wang M, Hauberg ME, Fullard JF, Kozlenkov A, Keenan A, et al. Brain Cell Type Specific Gene Expression and Co-expression Network Architectures. Sci Rep. 2018;8(1):8868.
30. Feng W, Chen L, Nguyen PK, Wu SM, Li G. Single Cell Analysis of Endothelial Cells Identified Organ-Specific Molecular Signatures and Heart-Specific Cell Populations and Molecular Features. Front Cardiovasc Med. 2019;6:165.
31. Li JY, Boado RJ, Pardridge WM. Rat blood-brain barrier genomics. II. J Cereb Blood Flow Metab. 2002;22(11):1319-26.

32. Pardridge WM. Blood-brain barrier genomics. Stroke. 2007;38(2 Suppl):686-90.
33. Bangsow T, Baumann E, Bangsow C, Jaeger MH, Pelzer B, Gruhn P, et al. The epithelial membrane protein 1 is a novel tight junction protein of the blood-brain barrier. J Cereb Blood Flow Metab. 2008;28(6):1249-60.
34. Chaves C, Do TM, Cegarra C, Roudières V, Tolou S, Thill G, et al. Non-Human Primate Blood-Brain Barrier and In Vitro Brain Endothelium: From Transcriptome to the Establishment of a New Model. Pharmaceutics. 2020;12(10).
35. Chaves C, Campanelli F, Chapy H, Gomez-Zepeda D, Glacial F, Smirnova M, et al. An Interspecies Molecular and Functional Study of Organic Cation Transporters at the Blood-Brain Barrier: From Rodents to Humans. Pharmaceutics. 2020;12(4).
36. Perrière N, Demeuse P, Garcia E, Regina A, Debray M, Andreux JP, et al. Puromycin-based purification of rat brain capillary endothelial cell cultures. Effect on the expression of blood-brain barrier-specific properties. J Neurochem. 2005;93(2):279-89.
37. Perrière N, Yousif S, Cazaubon S, Chaverot N, Bourasset F, Cisternino S, et al. A functional in vitro model of rat blood-brain barrier for molecular analysis of efflux transporters. Brain Res. 2007;1150:1-13.
38. Uchida Y, Ohtsuki S, Katsukura Y, Ikeda C, Suzuki T, Kamiie J, et al. Quantitative targeted absolute proteomics of human blood-brain barrier transporters and receptors. J Neurochem. 2011;117(2):333-45.
39. Ito K, Uchida Y, Ohtsuki S, Aizawa S, Kawakami H, Katsukura Y, et al. Quantitative membrane protein expression at the blood-brain barrier of adult and younger cynomolgus monkeys. J Pharm Sci. 2011;100(9):3939-50.
40. Li JY, Boado RJ, Pardridge WM. Blood-brain barrier genomics. J Cereb Blood Flow Metab. 2001;21(1):61-8.
41. Enerson BE, Drewes LR. The rat blood-brain barrier transcriptome. J Cereb Blood Flow Metab. 2006;26(7):959-73.
42. Daneman R, Zhou L, Agalliu D, Cahoy JD, Kaushal A, Barres BA. The mouse blood-brain barrier transcriptome: a new resource for understanding the development and function of brain endothelial cells. PLoS One. 2010;5(10):e13741.
43. Badhwar A, Stanimirovic DB, Hamel E, Haqqani AS. The proteome of mouse cerebral arteries. J Cereb Blood Flow Metab. 2014;34(6):1033-46.
44. Chun HB, Scott M, Niessen S, Hoover H, Baird A, Yates J, 3rd, et al. The proteome of mouse brain microvessel membranes and basal lamina. J Cereb Blood Flow Metab. 2011;31(12):2267-81.
45. Tam SJ, Richmond DL, Kaminker JS, Modrusan Z, Martin-McNulty B, Cao TC, et al. Death receptors DR6 and TROY regulate brain vascular development. Dev Cell. 2012;22(2):403-17.
46. Boado RJ, Li JY, Wise P, Pardridge WM. Human LAT1 single nucleotide polymorphism N230K does not alter phenylalanine transport. Mol Genet Metab. 2004;83(4):306-11.

47. Shusta EV, Boado RJ, Mathern GW, Pardridge WM. Vascular genomics of the human brain. J Cereb Blood Flow Metab. 2002;22(3):245-52.
48. Shawahna R, Uchida Y, Decleves X, Ohtsuki S, Yousif S, Dauchy S, et al. Transcriptomic and quantitative proteomic analysis of transporters and drug metabolizing enzymes in freshly isolated human brain microvessels. Mol Pharm. 2011;8(4):1332-41.
49. Jones AR, Stutz CC, Zhou Y, Marks JD, Shusta EV. Identifying blood-brain-barrier selective single-chain antibody fragments. Biotechnol J. 2014;9(5):664-74.
50. Muruganandam A, Tanha J, Narang S, Stanimirovic D. Selection of phage-displayed llama single-domain antibodies that transmigrate across human blood-brain barrier endothelium. FASEB J. 2002;16(2):240-2.
51. Stutz CC, Zhang X, Shusta EV. Combinatorial approaches for the identification of brain drug delivery targets. Curr Pharm Des. 2014;20(10):1564-76.
52. Farrington GK, Caram-Salas N, Haqqani AS, Brunette E, Eldredge J, Pepinsky B, et al. A novel platform for engineering blood-brain barrier-crossing bispecific biologics. The FASEB Journal. 2014;28(11):4764-78.
53. Li J, Meyer, A., Mäger, I.,Johansson, H.J., Lenter, M., Hildebrandt, T., Leparc, G., Untucht, C., Sim, J., Gumbleton, M., Plyte, S., Zhang, W., Letoha, T., El Andaloussi, S., Bell, R., Lesuisse, D., Wood, M.J.A. Manuscript in preparation. 2020.
54. Watts RJ, Dennis, M., Freskgard, P.O, Tam, S. WO. WO2011 091304 A1.
55. Morales-Alcala CC, Georgiou IC, Timmis AJ, Riobo-Del Galdo NA. Integral Membrane Protein 2A Is a Negative Regulator of Canonical and Non-Canonical Hedgehog Signalling. Cells. 2021;10(8):2003.
56. McKeown L, Robinson P, Greenwood SM, Hu W, Jones OT. PIN-G--a novel reporter for imaging and defining the effects of trafficking signals in membrane proteins. BMC Biotechnol. 2006;6:15.
57. Ehrlich M, Shmuely A, Henis YI. A single internalization signal from the di-leucine family is critical for constitutive endocytosis of the type II TGF-beta receptor. J Cell Sci. 2001;114(Pt 9):1777-86.
58. Bulut GB, Sulahian R, Ma Y, Chi NW, Huang LJ. Ubiquitination regulates the internalization, endolysosomal sorting, and signaling of the erythropoietin receptor. J Biol Chem. 2011;286(8):6449-57.
59. Jacobsen SE, Ammendrup-Johnsen I, Jansen AM, Gether U, Madsen KL, Bräuner-Osborne H. The GPRC6A receptor displays constitutive internalization and sorting to the slow recycling pathway. J Biol Chem. 2017;292(17):6910-26.
60. Helms HC, Abbott NJ, Burek M, Cecchelli R, Couraud PO, Deli MA, et al. In vitro models of the blood-brain barrier: An overview of commonly used brain endothelial cell culture models and guidelines for their use. J Cereb Blood Flow Metab. 2016;36(5):862-90.
61. Urich E, Lazic SE, Molnos J, Wells I, Freskgard PO. Transcriptional profiling of human brain endothelial cells reveals key properties crucial for predictive in vitro blood-brain barrier models. PLoS One. 2012;7(5):e38149.

62. Masuda T, Hoshiyama T, Uemura T, Hirayama-Kurogi M, Ogata S, Furukawa A, et al. Large-Scale Quantitative Comparison of Plasma Transmembrane Proteins between Two Human Blood-Brain Barrier Model Cell Lines, hCMEC/D3 and HBMEC/ciβ. Mol Pharm. 2019;16(5):2162-71.
63. Stanimirovic DB, Bani-Yaghoub M, Perkins M, Haqqani AS. Blood-brain barrier models: in vitro to in vivo translation in preclinical development of CNS-targeting biotherapeutics. Expert Opin Drug Discov. 2015;10(2):141-55.
64. Haqqani AS, Delaney CE, Brunette E, Baumann E, Farrington GK, Sisk W, et al. Endosomal trafficking regulates receptor-mediated transcytosis of antibodies across the blood brain barrier. J Cereb Blood Flow Metab. 2018;38(4):727-40.
65. Chang HY, Morrow K, Bonacquisti E, Zhang W, Shah DK. Antibody pharmacokinetics in rat brain determined using microdialysis. MAbs. 2018;10(6):843-53.
66. Pepinsky RB, Shao Z, Ji B, Wang Q, Meng G, Walus L, et al. Exposure levels of anti-LINGO-1 Li81 antibody in the central nervous system and dose-efficacy relationships in rat spinal cord remyelination models after systemic administration. J Pharmacol Exp Ther. 2011;339(2):519-29.
67. Pardridge WM. Blood-Brain Barrier and Delivery of Protein and Gene Therapeutics to Brain. Front Aging Neurosci. 2019;11:373.
68. Goldenring JR. Recycling endosomes. Curr Opin Cell Biol. 2015;35:117-22.

Figures

Figure 1

ITM2A mRNA quantification by RNAseq from http://www.brainrnaseq.org/ ITM2A mRNA is highly represented in mouse (upper graph) and human (lower graph) brain endothelial cells(28).Copyright from Steven Sloan.

Figure 2

Flowchart for full validation of ITM2A as a potential brain delivery target. Go steps are highlighted with blue arrow, no-go steps are highlighted with red arrow.

Figure 3

Human or mouse tagged ITM2A plasmid design. Each construct has intracellular domain (ICD) in blue, transmembrane domain (TM) in yellow and ECD in green with brichos domain. 3A: HA tag localisation in red, 3B: GFP tag in fluo green and wt construct.

Figure 4

Human or mouse GFP tagged ITM2A expression in HEK293 cells. HEK293 cells are stably recombined with human or mouse ITM2A with GFP tag at different positions. GFP tag ITM2A is visualized in green, and nuclei are stained in blue by Hoechst.

Figure 5

Highlighting the ITM2A colocalization with HEK293 human ITM2A N-Ter GFP cell compartments. A: confocal images of N-Ter GFP ITM2A in green and antibody anti-Giantin (ab37266) in red B: confocal images of N-Ter GFP ITM2A in green and antibody anti-LAMP1 (ab24170) in red. Yellow color indicates colocalization in the same focal plan, red and green colors indicate no colocalization in the same focal plan.

Figure 6

HEK293 human ITM2A uptake and internalization of several antibodies (anti-ITM2A, anti-GFP or anti-HA). A : HEK293 ITM2A wt, ITM2A GFP N-Ter and ITM2A GFP C-Ter : internalization of anti ITM2A AF4876 revealed with anti-Rabbit Alexa 647 in red; B : HEK293 ITM2A wt, ITM2A GFP N-Ter and ITM2A GFP C-Ter : internalization of anti ITM2A 14407-1-AP revealed with anti-Rabbit Alexa 647 in red, C : HEK293 ITM2A wt, ITM2A GFP N-Ter and ITM2A GFP C-Ter : internalization of anti GFP A31852 Alexa 647 in red; D : HEK293 ITM2A GFP N-Ter and ITM2A GFP C-Ter : internalization of anti GFP A31852 revealed with anti-Rabbit Alexa 647 in red E : HEK293 ITM2A HA N-Ter and ITM2A HA C-Ter : internalization of anti HA 901509 Alexa 488 in green.

Figure 7

HEK293 mouse ITM2A uptake of anti-GFP Antibodies. Internalization of anti GFP A31852 revealed with anti-Rabbit Alexa 647 in red

Figure 8

Anti-ITM2A antibodies internalization. A: Anti ITM2A Yumab G04 internalization with 3 different constructions in HEK293 cells expressing human ITM2A B: Anti ITM2A Yumab 93- G04, 147-A01, 147-E02 & 147-H07 cell internalization in HEK293 cells expressing human N-Ter GFP ITM2A

Figure 9

ITM2A RNA detection in mouse and monkey endothelial cells. P0D0 = fresh microvessels, P0D7 = endothelial cells after 1 week in culture, P1D7 = endothelial cells after 1 thawing then 1 week in culture. A: ITM2A mRNA levels in the monkey brain endothelium from cortex analyzed with RNA seq at different time of culture. B: Differences in the mRNA levels of itm2a and CD31 in mouse endothelial cells. CD31 in orange and itm2a in blue. Microvessels named P0D0, primary cells selected by puromycin named P0D7, primary cells selected by CD31+ named P0D0 CD31+ selected and P0D7 CD31+selected. Housekeeping gene used was actin.

Figure 10

Immunofluorescence staining of mouse ITM2A protein in rodent endothelial cells with three ITM2A antibodies. Labelling is visualized with secondary antibodies anti-human or rabbit with Alexa 647. Nuclei are labelled with Hoechst in blue. Immunolabelling has shown no or non-specific signal in primary cells contrary to HEK293 overexpressing ITM2A. Similarly, we could not detect endogenous ITM2A protein in hCMEC/D3 by immunolabelling compared to TFRC probably due to the downregulation of ITM2A in culture (Fig. 11)

Figure 11

Immunofluorescence staining of hCMEC/D3 with TFRC and ITM2A antibodies. Labelling is visualized with secondary antibodies anti human Alexa 647 in red. Nuclei are labelled with Hoechst in blue.

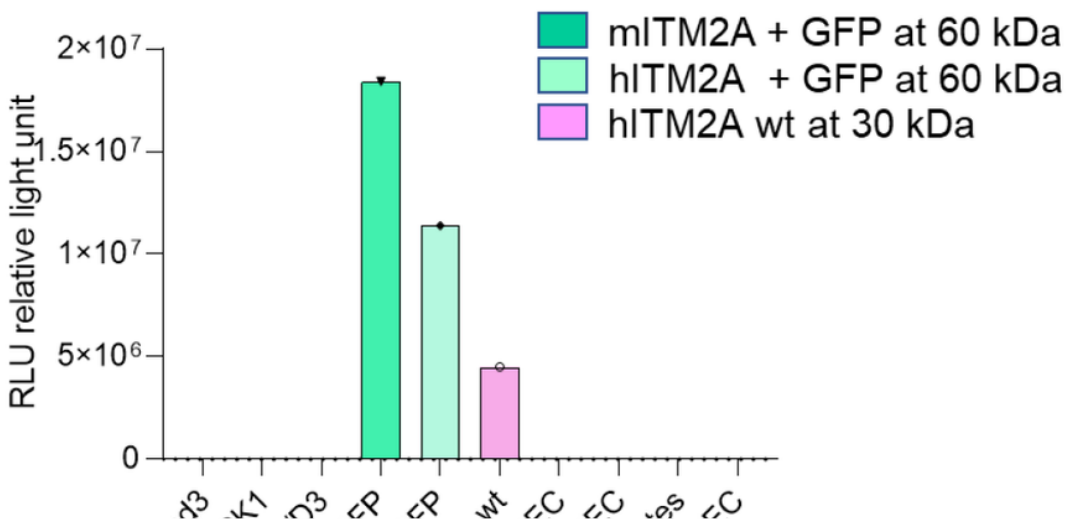

Figure 12

Relative quantification of ITM2A protein expression in different cells by Western Blot. In green protein quantification at 60 kDa (ITM2A + GFP) in pink protein quantification at 30 kDa (ITM2A). Western Blot membranes are in additional file 2.

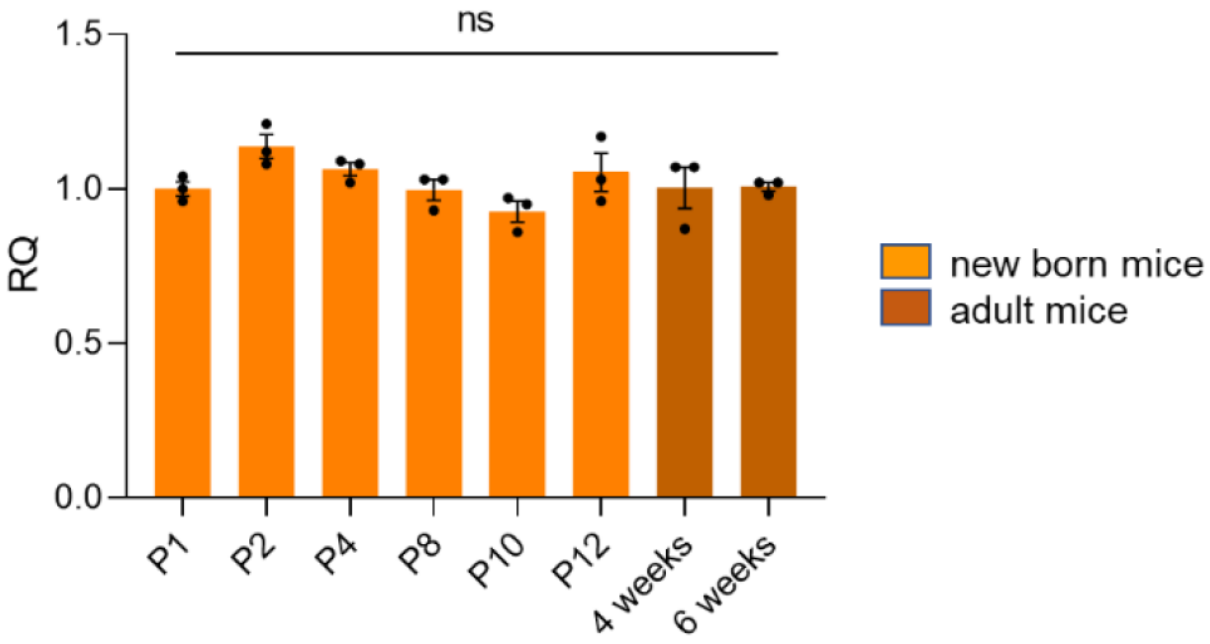

Figure 13

itm2a mRNA relative quantity (RQ) in new-born and adult mice brain homogenate. Housekeeping gene was gapdh. Results are expressed as mean ± S.D. (n = 1 experiment, performed in triplicates). P-values were obtained by Ordinary One-way ANOVA with Dunnett's multiple comparisons test vs P1 ns: no statistical significance = $p > 0.05$.

Figure 14

Relative quantification of ITM2A protein expression in newborn mice by Western Blot. HEK293 mouse ITM2A GFP is used as control. In green protein quantification at 60 kDa (ITM2A + GFP) in pink protein quantification at 30 kDa (ITM2A) using antibody anti-ITM2A AF4876. Western Blot membranes in additional file 3

Figure 15

Quantification of ITM2A in samples of cells and tissues from mice by LC/MS. LC/MS Cortex results are in purple, Muscle results in blue and cells results in green. Results are expressed as mean ±S.D. (3 quantified peptides). P-values were obtained by Ordinary One-way ANOVA with Kruskal-Wallis multiple comparisons test vs Cortex P1 or Muscle P1 or by Mann-Whitney test for comparison between Cortex Adult and Brain microvessels ns: no statistical significance = p > 0.05.

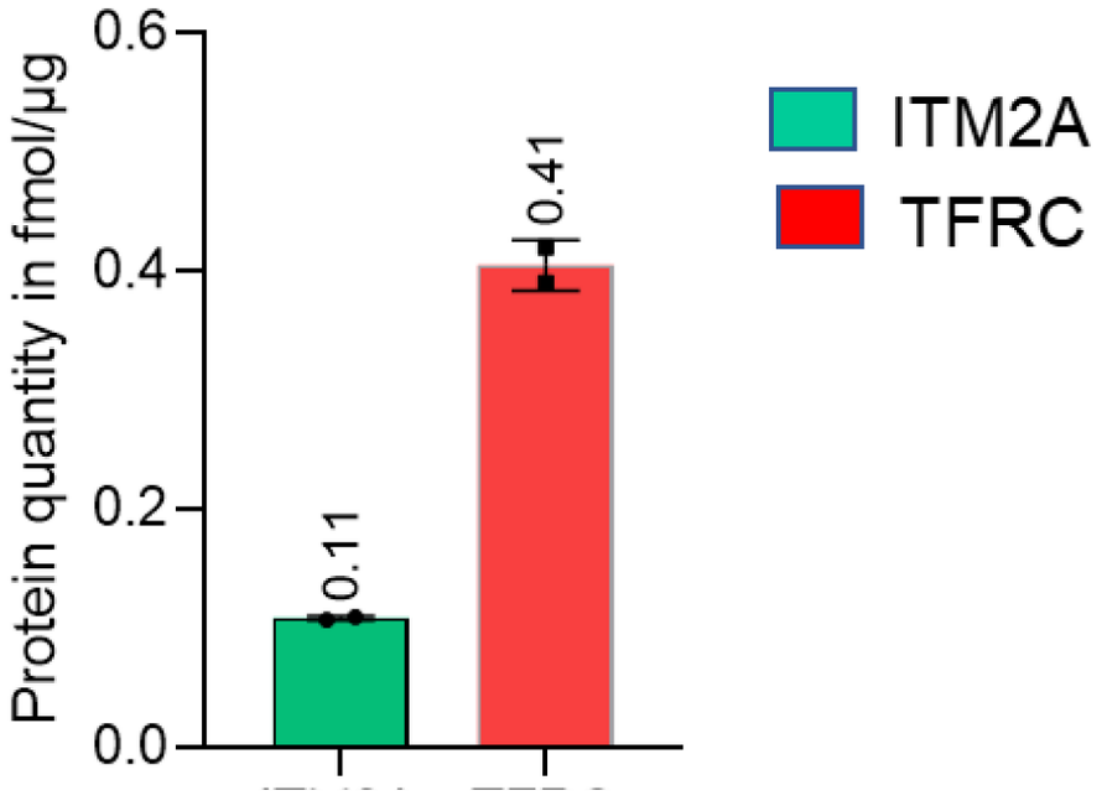

Figure 16

Quantification of ITM2A in samples of brain microvessels from human by LC/MS. Protein quantification results for ITM2A are in green and for TFRC are in red. Results are expressed as mean ±S.D. (4 quantified peptides for ITM2A and 5 quantified peptides for hTFRC).

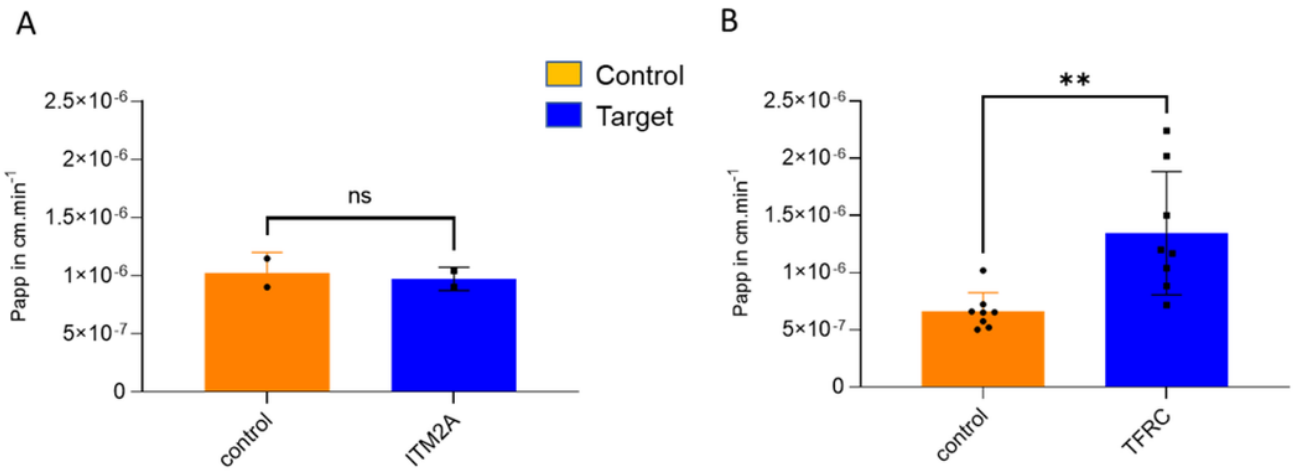

Figure 17

In vitro human brain transcytosis model from Brainplotting. Control mouse IgG in orange and antibodies anti-target in blue ITM2A (Fig. 17A) or TFRC (Fig. 17B) were incubated together in apical compartment of transwell seeded with primary human endothelial cells. Basolateral medium was analyzed by ELISA to quantify antibodies transport. Results are expressed in means ± Standard Deviation p-values were obtained by Mann-Whitney test ns: no statistical significance = $p > 0.05$ for ITM2A antibody and unpaired t-test ** = $p < 0.01$ for TFRC antibody

Figure 18

In vivo mouse brain exposure of an ITM2A monoclonal antibody. 5 mpk iv injection of G04 and anti-TNP to C57Bl6 mice; samples were collected 5h after injection. ELISA assay: capture with F(ab')2 monkey anti-human IgG1 Fc fragment, detection with Goat anti-human sulfo-tagged 1/100. Results are expressed as mean ± S.D. (n = 1 experiment, performed in triplicate, 3 animals). P-values were obtained by Two-way ANOVA with Sidak's multiple comparisons test ns: no statistical significance = $p > 0.05$, **** = $p < 0.0001$

Supplementary Files

This is a list of supplementary files associated with this preprint. Click to download.

- Additionalfile1.docx
- Additionalfile2.docx
- Additionalfile3.docx
- Additionalfile4.docx